Flying Sensors for Monitoring Green Water Credits

Location:
SE-Spain

Flight dates:
6-Jul – 9-Jul 2015

Authors:
Johannes Hunink
Peter Droogers
Jan van Til
Godert van Lynden

Client:
2g@there Netherlands-Algeria Water Collaboration project

HiView
Costerweg 1V
6702AA Wageningen
www.hiview.nl
info@hiview.nl
0317 460050

Contents

1 Introduction

Green Water Credits (GWC) is an investment mechanism that supports upstream land and water users to improve water resources management for the benefit of all water users in a catchment. The funds for these payments are coming from the extra benefits of the downstream water users. A pilot project is currently conducted by ISRIC, FutureWater and partners to demonstrate and evaluate the possibilities of implementing Green Water Credits in the Oued de la Mina, which is a catchment of the Cheliff Basin in Northern Algeria.

Monitoring the impact of GWC practices on erosion control and vegetation is key to the success of any GWC project. Traditionally, monitoring is done at looking at streamflows and sediments loads, before and after implementation. However, with the advance in Flying Sensors techniques (sometimes referred to as drones or UAVs), detailed information on the stage of erosion can be obtained.

Overall, Flying Sensors can support the design and implementation of Green Water Credits, by:

1. Spatial inventories of GWC practices:
    - Where certain practices take place?
    - How do they change over time?
    - Where adoption takes place, where not?
    - Where are the “early adopters”?
    - Diffusion of practices
2. Assess implementation properties of GWC practices
    - Slope degree,
    - Strip width, terrace intervals
    - Tillage and contours
3. Monitoring effectiveness of GWC practices
    - Soil moisture, soil organic matter
    - Where do rills occur, does their appearance reduce/increase?
    - Gullies – how do they evolve over time? Are they active, and which parts are most active?
    - Monitoring landscape fragmentation and monitoring of habitats degradation.
    - Monitoring of downstream water use, water consumption, water quality

GWC is currently explored and tested in various countries. For the case in Algeria specific interest exists in using Flying Sensors. Because of some practical constraints the methodology was tested and demonstrated in an area with similar environmental settings as the Cheliff Basin. For the Segura Basin in Southern Spain has been used.

2 Sites

A total of 8 sites were explored and are summarized hereafter.

Site code	150706 – A
Description	Experimental farm Universidad Politécnica de Cartagena (UPCT) and surrounding agricultural fields (downstream in basin)
Day of flight	6-Jul-15
Coordinates	0.94; 37.68
Area	
Crops	Almond, vineyard, Cereals, melons, pepper
Farmer practices	Regulated deficit irrigation, drip irrigation

Location

Photos

Raw Flying Sensor images

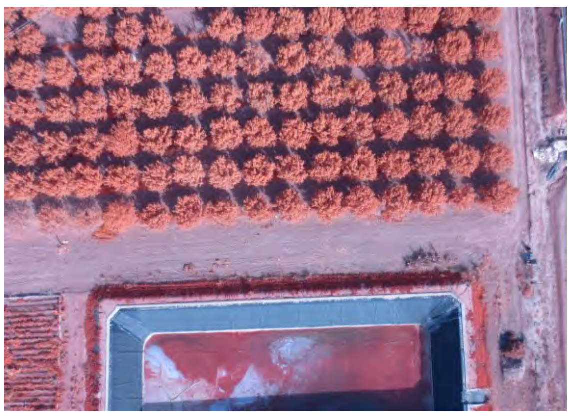

Site code	150706 – B
Description	Commercial citrus farm Cerezuela in Campo de Cartagena district (mid-stream in basin)
Day of flight	6-Jul-15
Coordinates	0.92; 37.68
Area	
Crops	Oranges (Fortune)
Farmer practices	Drip irrigation

Location

Photos

Raw Flying Sensor images

Site code	150707 – C
Description	Commercial citrus farm and experimental farm of National Research Council (CEBAS – CSIC, lead: Emilio Nicolás) (mid-stream in basin)
Day of flight	7-Jul-15
Coordinates	1.21; 38.12
Area	
Crops	Mandarins and Grapefruit
Farmer practices	Drip irrigation, regulated deficit irrigation, irrigation with treated wastewater

Location

Photos

Raw Flying Sensor images

Site code	150708 – D	Location
Description	Los Alhagüeces farm, plot with rainfed almond trees with experiments of different tillage practices carried out by National Research Council (CEBAS – CSIC, lead: Joris de Vente) (upstream in basin)	
Day of flight	8-Jul-15	
Coordinates	1.72; 37.86	
Area		
Crops	Almonds	
Farmer practices	No tillage, reduced tillage, mulching	

Photos	Raw Flying Sensor images
	
	

Site code	150708 – E	Location
Description	Los Alhagüeces farm, cereal plot with experiments of different tillage practices carried out by National Research Council (CEBAS – CSIC, lead: Joris de Vente) (upstream in basin)	
Day of flight	8-Jul-15	
Coordinates	1.72; 37.86	
Area		
Crops	Cereals	
Farmer practices	Reduced tillage	

Photos	Raw Flying Sensor images
	
	

Site code	150708 – F
Description	Los Alhagüeces farm, SE-Spain, hillslopes with stone walls and almond trees. (upstream in basin)
Day of flight	8-Jul-15
Coordinates	1.73; 37.86
Area	
Crops	Almonds
Farmer practices	Stone walls, terracing

Location

Photos

Raw Flying Sensor images

HiView

Site code	150709 – G
Description	Los Alhagüeces farm, SE-Spain, Almond trees with rainwater harvesting system (upstream in basin)
Day of flight	9-Jul-15
Coordinates	1.71; 37.83
Area	
Crops	Almonds
Farmer practices	Terracing, rainwater harvesting

Location

Photos

Raw Flying Sensor images

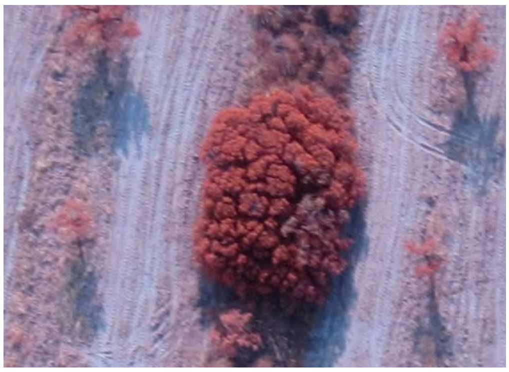

Site code	150709 – H
Description	Los Alhagüeces farm, SE-Spain, reforested area with old almond trees with gully systems (upstream in basin)
Day of flight	9-Jul-15
Coordinates	1.72; 37.82
Area	
Crops	Almonds, reforestation with pine trees, and cereals
Farmer practices	Terracing, reforestation

Location

Photos

Raw Flying Sensor images

3 Methodology

3.1 Unmanned Aerial Vehicle

One of HiView's Flying Sensors has been used for the study. The Flying Sensor is a fixed-wing one that has a wingspan of 96 cm and a take-off capacity of 0.7 kg. It is capable of approximately 40 minute flights at cruise speeds of around 50 km/h and can be flown either manually or using an autopilot. The Flying Sensor has an autopilot that follows the waypoints of a flight plan created using flight planner software. A constant radio link between the flight planner software and the Flying Sensor allows for inflight monitoring and control. The Flying Sensor is mounted with a GPS receiver, altimeter, wind meter and a sensor that is electronically triggered by the autopilot system to acquire images at the correct positions.

Two sensors were used: one for the visible light spectrum, and one including the near infrared spectral region (NIR). The sensors have a 16 megapixel sensor, i.e. 4608 by 3456 pixels, and capture JPEG format images. Its lens is capable of focal lengths between 4.3 and 21.5 mm. It is fixed at 4.3 mm, however, to minimize potential motion blur as well as to allow faster shutter speeds by maximizing the amount of sensed light. During surveys the camera is set to full-auto mode in which the device uses autofocus and automatically chooses the appropriate combination of aperture, ISO and shutter speed for the given light condition. In sufficiently light conditions the full-auto setting generally results in images captured with relatively large apertures, ISO values in the 125-250 range and shutter speeds of 1/320-1/1200 seconds.

3.2 Digital elevation model

The Flying Sensor images were processed into ortho-photos and grid-based DEMs of the different sites using a Structure from Motion (SfM) workflow [*Lucieer et al.*, 2013]. The SfM process starts by selection of the images with sufficient overlap from multiple positions and/or angles and quality. Blurred images are removed where redundant. Next, an image feature recognition algorithm is used to automatically detect and match characteristic image objects between photographs, i.e. the scale invariant feature transform (SIFT) described by Lowe (2004). A bundle block adjustment is then performed on the matched features to identify the 3D position and orientation of the cameras, and the xyz location of each feature in the images resulting in a sparse 3D point cloud [*Triggs et al.*, 2000; *Snavely et al.*, 2007; *Plets et al.*, 2012; *Fonstad et al.*, 2013]. A densification technique is applied to derive dense 3D models using multi-view stereopsis (MVS) or depth mapping techniques (Furukawa & Ponce, 2009). The use of ground control points (GCPs) and/or incorporation of camera GPS locations allows for the georeferencing of the 3D model in a coordinate system. Finally, the model is exported to a high-resolution grid-based DEM and ortho-mosaics are derived based on the projected and blended photograph at a final resolution of 0.2 m and 0.1 m, respectively. In this study, we adopted the SfM workflow as implemented in the software package Agisoft PhotoScan Professional version 0.9.1[*Agisoft*, 2013]. The specific algorithms implemented in Photoscan are not detailed in the manual but a description of the SfM procedure in Photoscan and commonly used parameters are described in Verhoeven (2011).

3.3 Sensors and vegetation indices

From the Flying Sensor imagery, crop vegetation indices can be calculated. Vegetation indices measure the variation in crop vitality and biomass. Stress factors such as water and nutrient deficiencies can be made visible using these indices. There are many sensors available that differ in in the amount of spectral bands, band-width, noise correction, etc. Critical is the effect of saturation, making the sensors for a certain amount of biomass insensitive to changes in the chlorophyll content.

A wide range of vegetation indices have been developed, and related to crop status. Some of them are more widely applicable, other more focused on a particular crop growth characteristic. Some vegetation indices are designed to get a measure of the amount of biomass of a crop (NDVI, WDVI), other indices say something about the chlorophyll and nitrogen in the leaf. So, to monitor various crop parameters also different vegetation indices are needed.

A good indication for the vegetative condition is obtained by deriving the Normalized Difference Vegetation Index (NDVI). Vegetation gives a strong reflection in the range of 0.7-0.9 microns (near infrared), while a weak reflection in the range of 0.6-0.7 microns (red) due to the absorption by chlorophyll. The normalized difference in near-infrared and red is called NDVI. The NDVI values may lie in theory between the -1 and +1. In practice, values for bare ground are around 0.2 and for good growing vegetation around 0.8.

5 Inventory of Various GWC Practices

5.1 Methods and resolution

The aim of financial mechanisms like Green Water Credits (GWC) is to promote Sustainable Land Management (SLM) in upstream areas to positively influence water availability and water quality for downstream water users while at the same time sustaining livelihoods of upstream farmers. Farmers that implement the SLM practices are incentivized by direct economic compensation and/or indirect (crop yield) benefits.

Critical to successful implementation of GWC is the mobilization of the main private and public actors in the basin. This engagement requires high-quality information on the status of current land management (baseline) and changes in land management from the start of implementation. These changes include those that are promoted through GWC, but also external changes.

To assess the baseline conditions, and monitor land management changes, several methods can be employed:

- Farmer surveys based on a representative group of communities
- GIS mapping using satellite data with ground-truth data
- Flying Sensors to monitor the adoption, the implementation and the effectiveness of practices

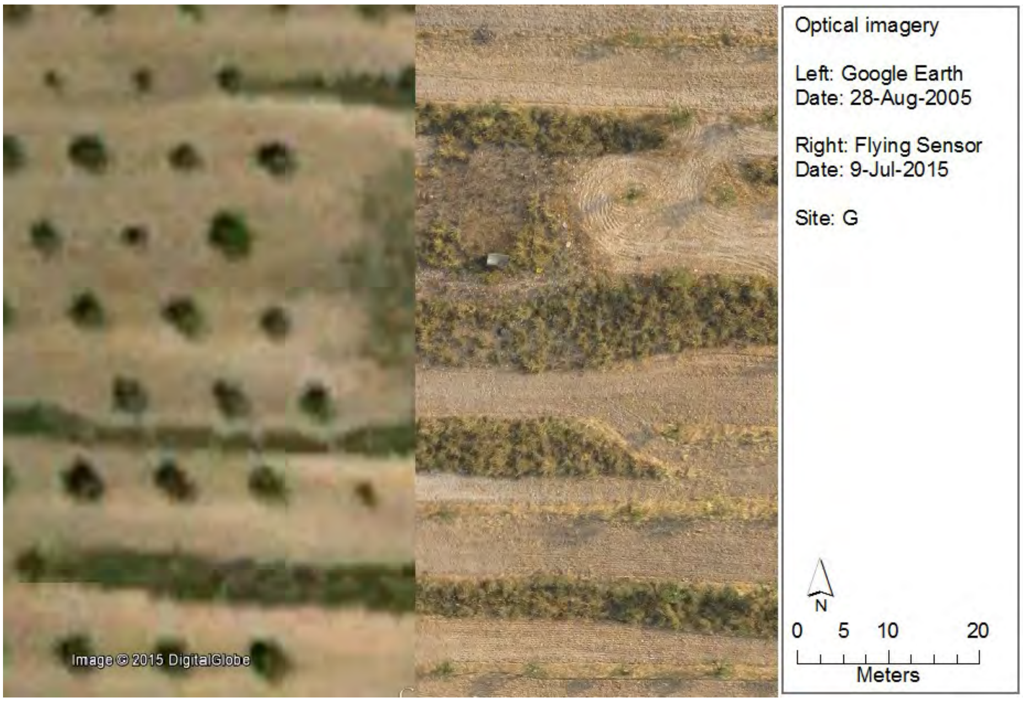

Figure 1. Google imagery (left) compared to Flying Sensor imagery (right) for the same site.

Farmer surveys can yield information on a wide range of relevant variables, both biophysical as socio-economic, and are useful to understand how farmers perceive the relationship between land management and downstream issues. This is key to the design of a successful incentive mechanism. A limitation of this methodology is that it is generally difficult to extract (un-biased) quantitative measures (location, extent, implementation levels) from the surveyed biophysical information. Also it can be cumbersome to map practices from the surveyed data and relate them with other spatially variable information.

Satellite-based GIS mapping of farmers´ practices and degradation status are often performed and have the advantage that they allow a large area to be mapped with relatively little effort and cost. Principal limitations are related to spatial resolution, and over-pass time (the date of the imagery).

A third option is to obtain information on the adoption of farmers´ practices by using Flying Sensors. They operate at an intermediate scale (between field-level and satellite) and take away several of the limitations of the above techniques:

- Provide ultra-high-resolution imagery, often necessary to understand how practices impact erosive patterns that occur on spatial resolutions < 10cm
- Allow a snapshot of the current situation whenever is desired, not dependent on available (clouds) and costly high-resolution satellite imagery
- Provide an objective measure of the scale of implementation and allow a wide range of useful properties on the implementation to be extracted.

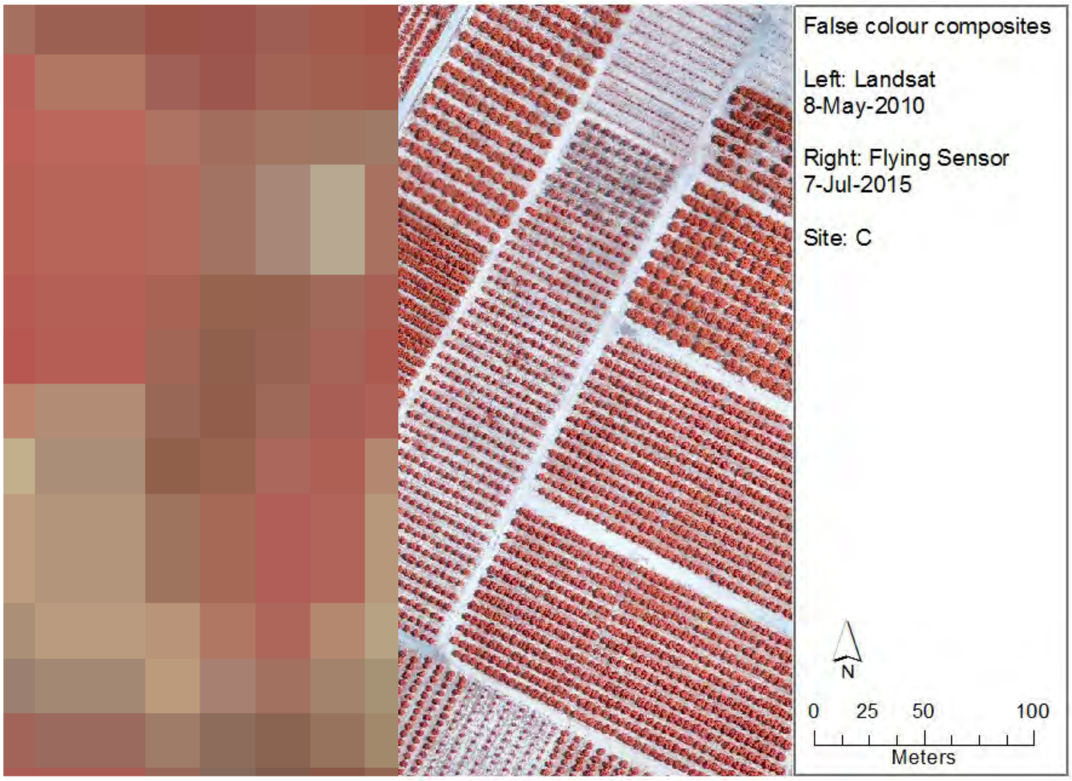

Figure 2. Comparison between Landsat imagery (left) and Flying Sensor imagery (right) of the same site (C) as so-called false-color composite.

To illustrate the difference in spatial resolution between freely available remote sensing imagery, the Figure 1 and Figure 2 show a comparison between

1. Google Earth imagery and Flying Sensor imagery. Available imagery through Google is often out-dated. Another disadvantage is that it does not allow downloading geo-referenced imagery and using it for post-processing analysis
2. Landsat false colour and Flying Sensor false colour imagery (so including the Near Infrared spectral range). Landsat is the satellite platform that provides the highest

resolution data which is freely available at this moment, including spectral bands in infrared and thermal. Resolution however is 1000 times coarser than what can be obtained using Flying Sensors (30 m compared to 3 cm). For comparison, the recently launched Sentinel platform by ESA is supposed to deliver maximum 5m resolution imagery, but most likely not for free at this resolution.

Also the digital elevation model that can be derived from the Flying Sensors is significantly more detailed than public domain datasets, explained in detail in section 6.1.

The following sections provide examples taken from the Flying Sensor flights for different sites across the Segura basin. A few relevant SLM technologies are highlighted.

5.2 Terraces

In semi-arid systems, there is wide variety of terrace types. The WOCAT database provides many examples in the Mediterranean area (e.g. database references T_SPA002en, T_TUN009en, T_GRE004en). Often these structural measures are combined with vegetative measures, such as grasses or trees. In the case of vegetative strips (ideally along slopes), these often lead to the gradual formation of bunds and terraces due to water erosion and/or 'tillage erosion' – the downslope movement of soil during cultivation.

Figure 3 shows for an area of site G that is partly terraced. The terraces can easily be identified from the contour lines (thin white lines) and the vegetative strips on the terrace edges. As can be seen, in the righter part of this image, terraces were not implemented, in spite of similar sloping conditions (distance between the contour lines is similar).

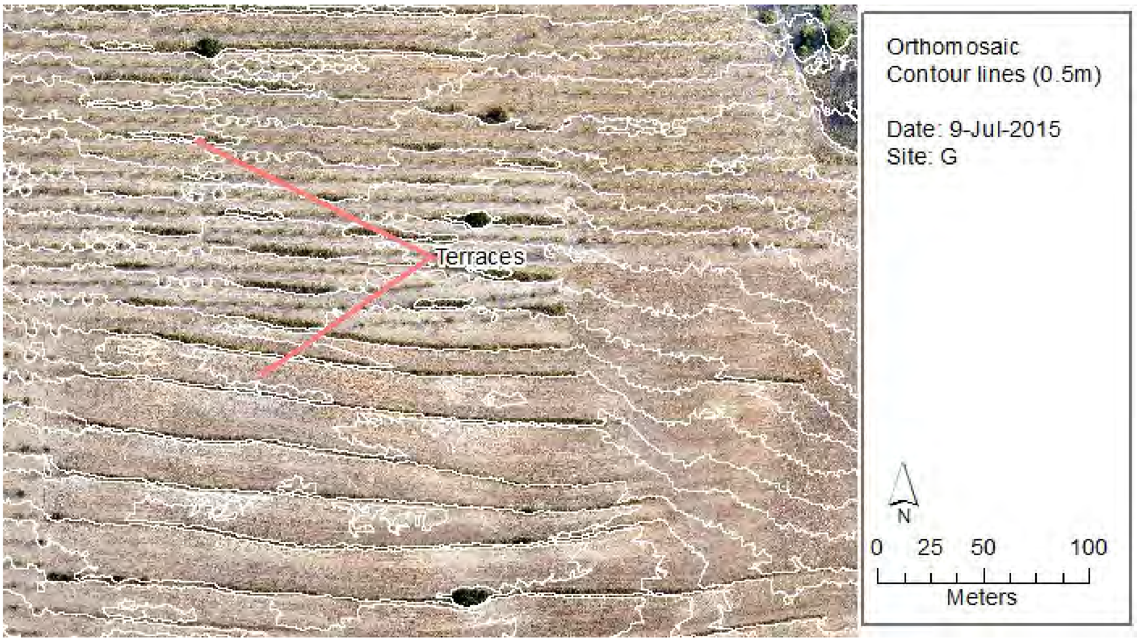

Figure 3. Identification of terraces from Flying Sensor derived orthomosaic and contour lines.

Mapping and identification of terraces can be done for larger areas in a semi-automated way using topographical indices and GIS techniques. Figure 4 shows the Terrain Ruggedness Index for the same area as in the previous figure. This index provides a quantitative measure of topographic heterogeneity. It is derived by calculating the sum change in elevation between a grid cell and its eight neighbour cells. As can be seen, terraces are easily identified as the longitudinal features in the image. The dotted features are the trees, which could be excluded using tree filtering algorithms.

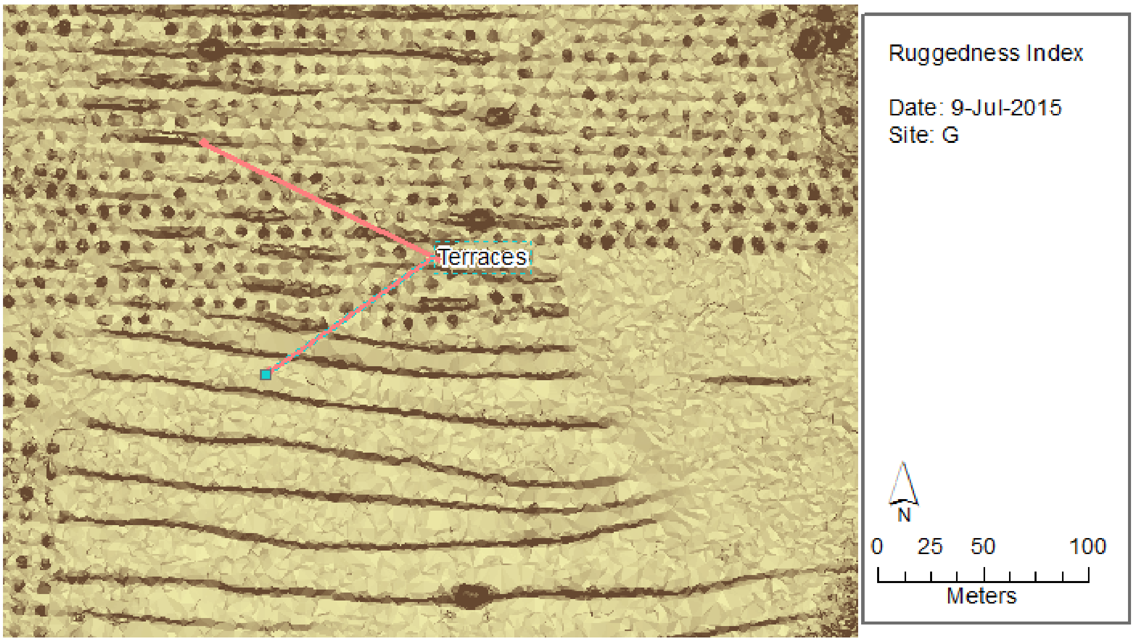

Figure 4. The Ruggedness Index for the same area as in Figure 3

5.3 Stone walls

Stone walls are common features in Mediterranean areas and often generate terraces due to the accumulation of sediments behind the barriers. Soil organic matter and soil humidity tends to increase and often farmers use this to plant fruit trees or annuals. The WOCAT database provides many examples of different types of Stone Wall terraces (e.g. WOCAT reference T_RSA003en and T_SYR001en). Also in this area, fruit trees (almonds) are planted just on the edge of the terraces, where soil moisture and organic matter content is highest.

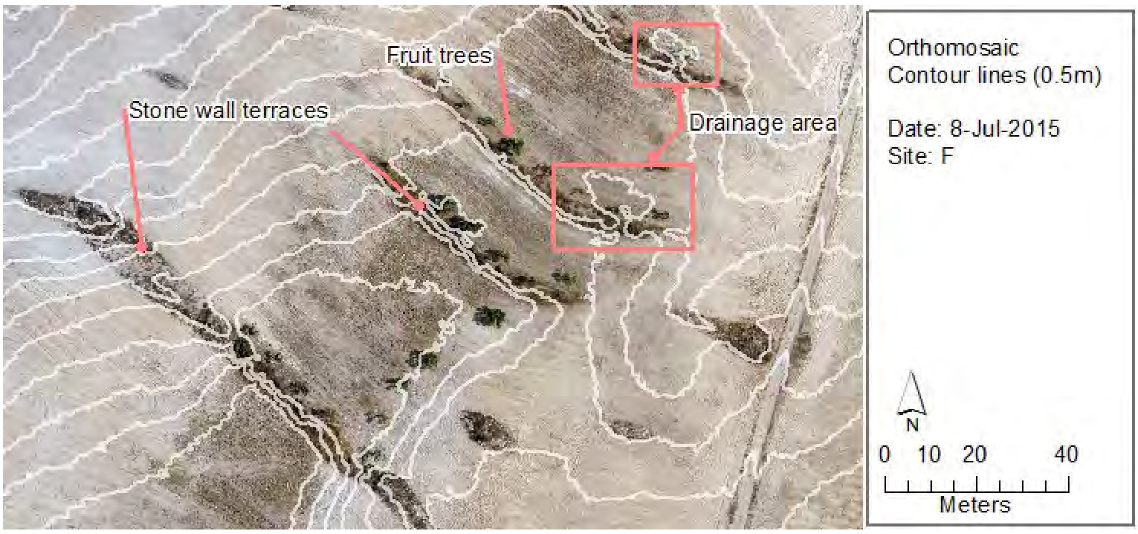

Figure 5. Stone wall terraces: high resolution imagery and contour lines based on Flying Sensors' hi-res digital elevation model.

Figure 5 shows Flying Sensor imagery from which trees and the stone walls (or gully plugs, which are shorter than stone walls) can be identified and mapped.

The same Figure 5 highlights the depression areas of the terraces in the upper right part of the image. The contour lines show that in these areas drainage occurs of the terraces during and after extreme rainfall events. This high-resolution information can thus help to identify weaknesses in the structural measures of SLM technologies.

5.4 Gully control

Gullies are common features in semi-arid systems and can cause significant loss of agricultural land, and contribute significantly to downstream sediment loads in the streams. Gully mitigation and control through a combination of conservation measures (vegetative, structural, management) is necessary to stabilize the gully system.

Figure 6 shows the high resolution elevation model of a gully system in a former almond grove that was afforested. As can be seen, the terraces can be easily identified in this high-resolution elevation model (straight darker lines). Since afforestation (around 5 years ago), no tillage took place in this plot, and the additional biomass is likely to stabilize the system. Multi-temporal analysis (with repeated flights) would be necessary to understand how the gully system evolves and what the main drivers behind its dynamics are.

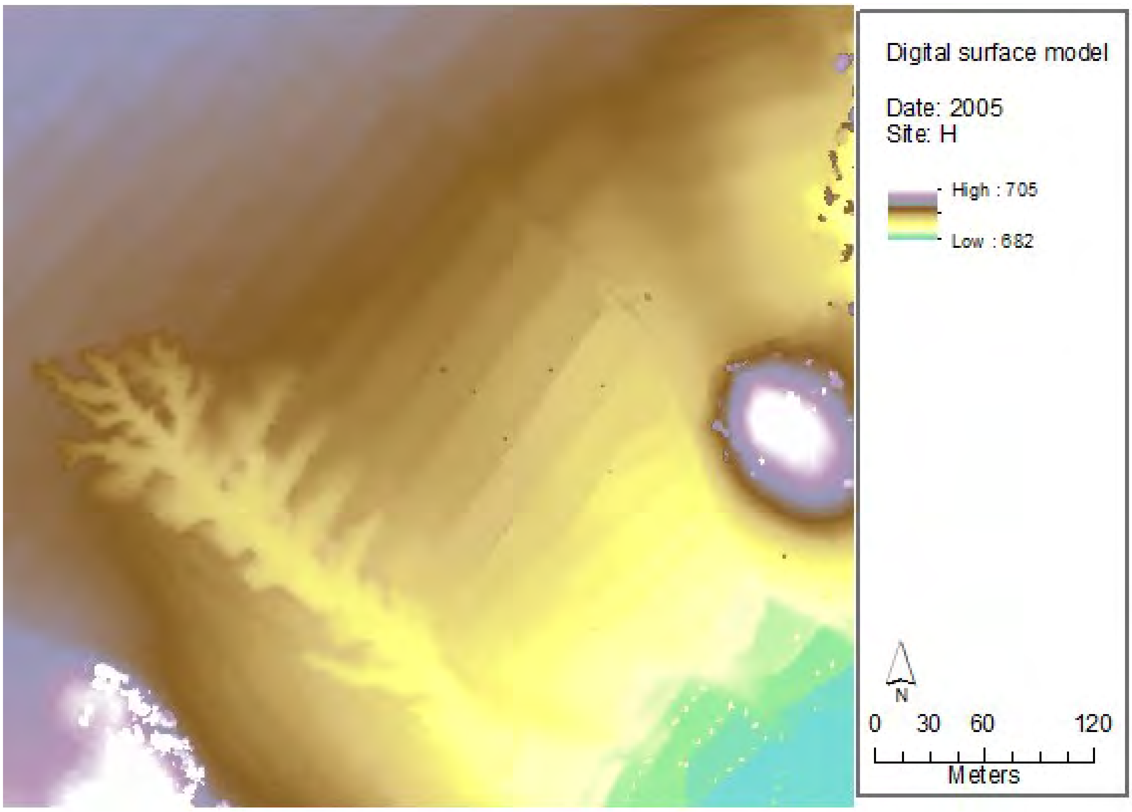

Figure 6. High resolution elevation model of a gully system.

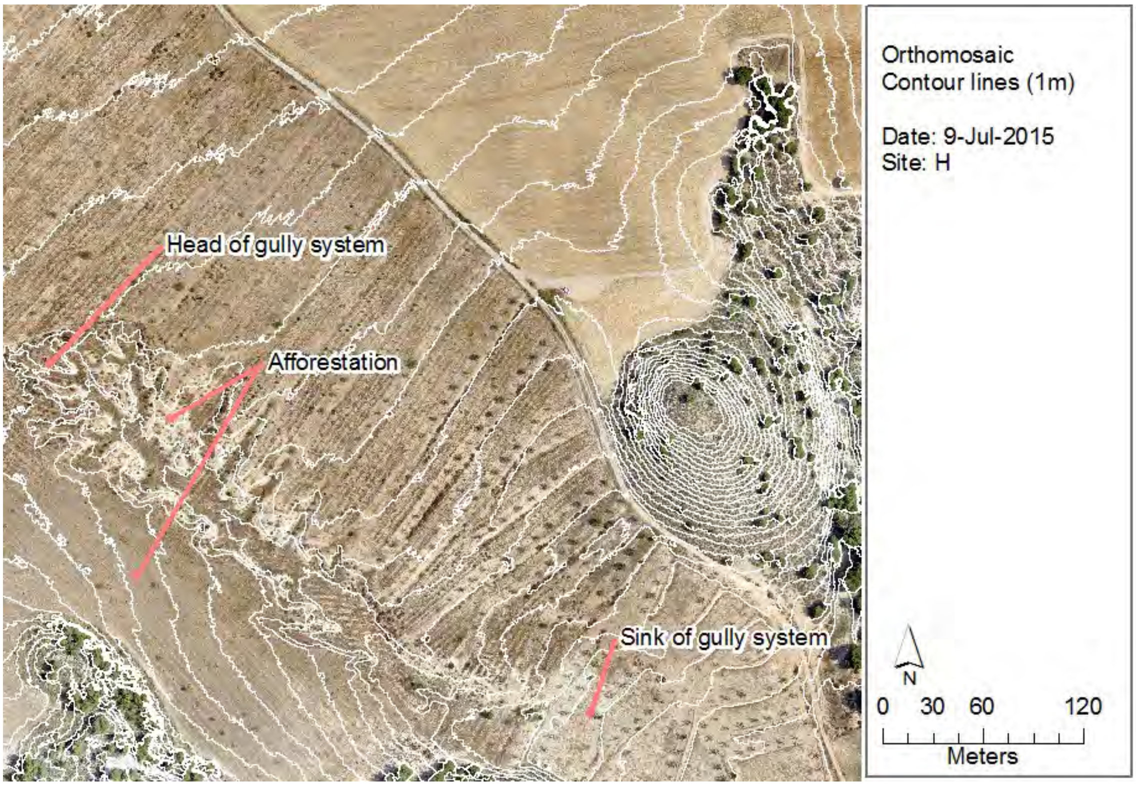

Figure 7. Orthomosaic and contour lines extracted from digital surface model of gully system

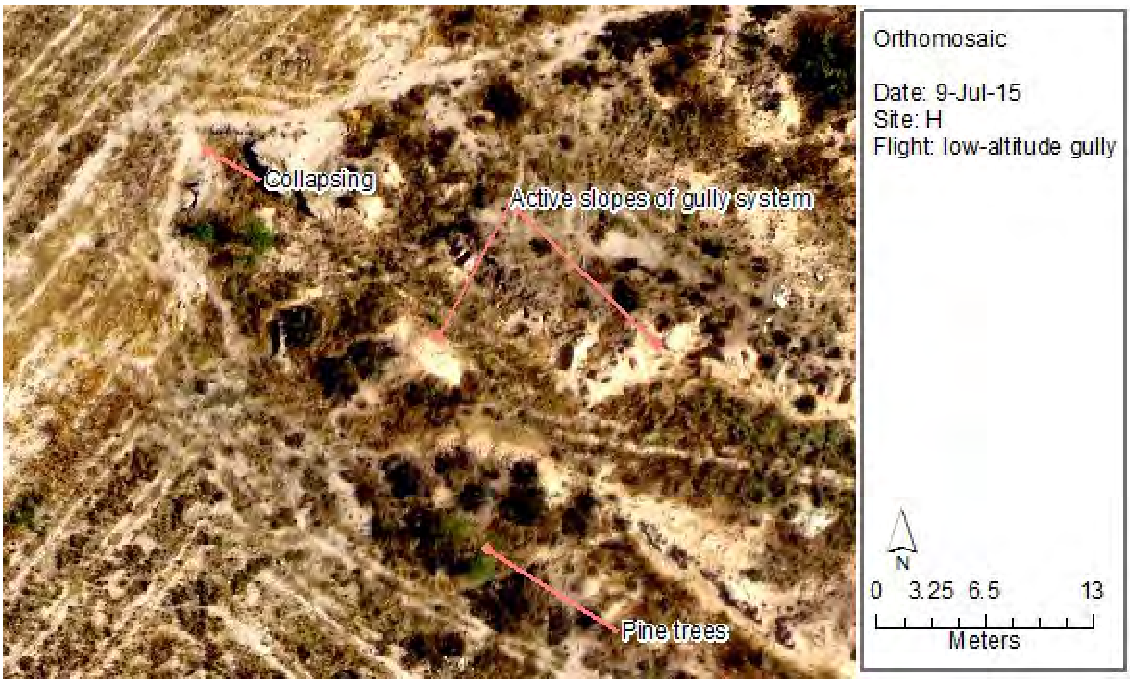

Figure 8. Detailed orthomosaic from additional low-altitude flight

Historic images can provide some insight in how the gully evolved over time, at least in extent. No low-cost data on elevation can be obtained, so for studying the morphological development of the gully additional Flying Sensors flight are useful. Figure 9 shows a screenshot of the same area from Google Earth. The latest imagery available on Google Earth are from 2005. The resolution of this imagery is considerably lower so for monitoring the evolution of specific features (gully heads, vegetation type, etc) in time this imagery is not sufficient. For studying how the extent evolved, a combination of historic Google Earth imagery and up-to-date Flying Sensor imagery can be attractive. In this case, the extent of the gully system has remained more or less the same, so apparently the system is relatively stable. The vegetation seems to have increased since then, probably due to the afforestation efforts.

Figure 9. Imagery from Google Earth from approximately the same area, but year 2005

6 Assess Implementation of GWC Practices

6.1 Resolution and surface elevation

The actual implementation of practices by farmers depends on local biophysical factors (slope, climate, soil, etc), economic constraints, farmers´ knowledge, etc. Monitoring how farmers actually implement the practices is necessary to make sure that they meet the objectives of GWC and generate the expected impact.

Also, to study impacts (past and future) through data analysis and simulation, it is often necessary to obtain detailed information on how practices are implemented. For example sloping direction of terraces, terrace length, direction of tillage, management measures related to grazing, etc.

To obtain useful spatial properties on the implementation of practices, a high resolution digital elevation model (or elevation model without vegetation) is critical. Obviously, for understanding the current situation, this elevation model should also be up-to-date. It may even be preferable to measure during a certain part of the year: just before planting, after harvest, or after the rainy season. Then, Flying Sensors are useful as they provide a low-cost means to generate high-resolution digital elevation models. Costs might be up to 10 times cheaper compared to classical surveying.

Figure 10 shows as example the comparison of the different resolutions of digital elevation models. The upper image is from satellite-based SRTM data (resolution 30m), freely available and often used for biophysical assessments for ecosystem services studies. The middle image is from LIDAR dataset. LIDAR can yield very high-resolution data but are very costly. The lower image shows for the same area the DEM obtained from the Flying Sensor flight (in this case 5 cm resolution).

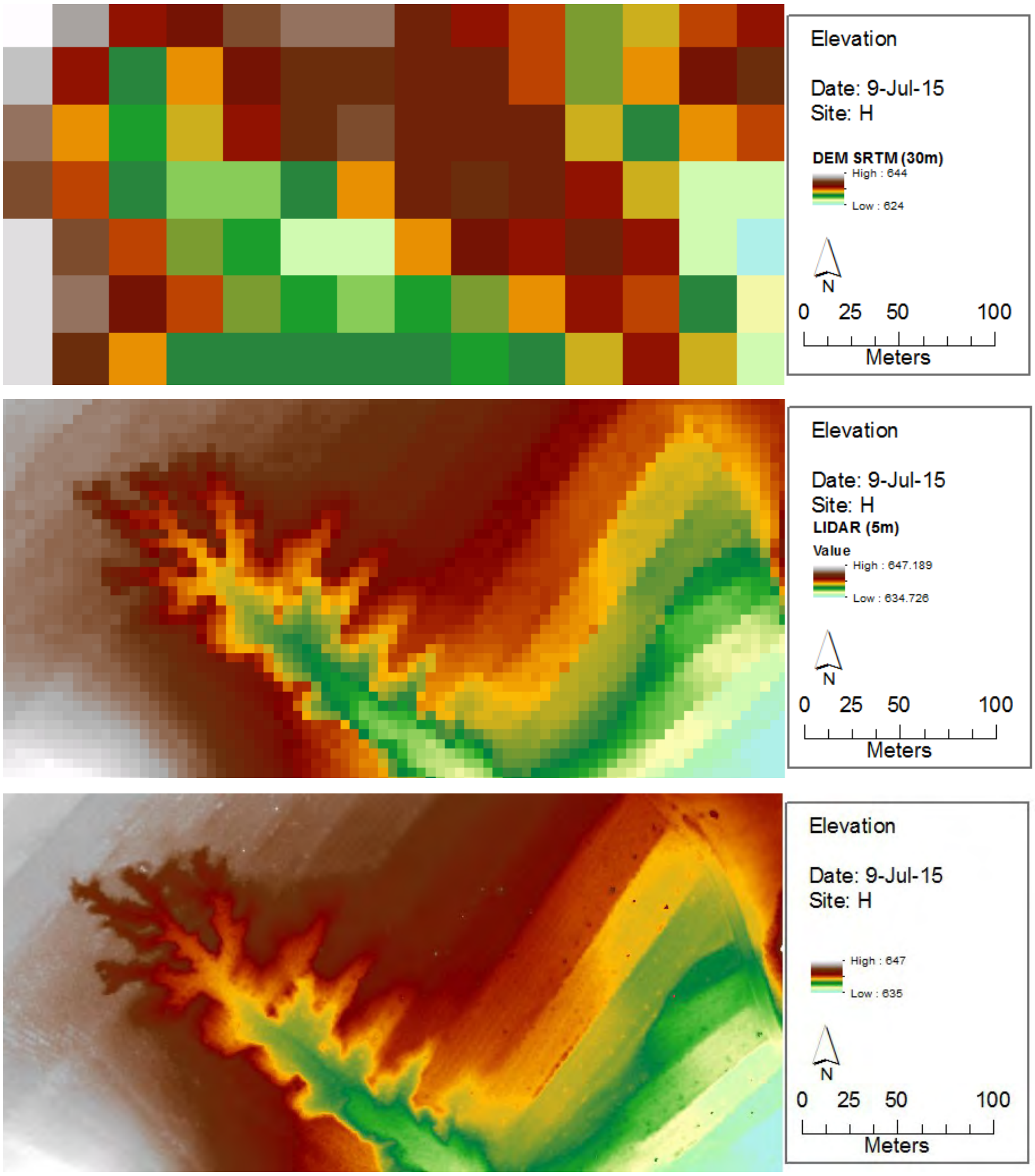

Figure 10. Comparison between digital elevation models from SRTM 30m (top), LIDAR (middle) and Flying Sensor (bottom).

The following sections provide some examples of how imagery and the high-resolution digital elevation model were used to obtain useful information on the implementation of several practices.

6.2 Slope

The key principle behind many SLM technologies is to divide a long slope of land into a series of shorter ones in order to reduce the runoff velocity and erosion. The example below compares a slope that was not terraced with the slope profile of a terraced area, with similar elevation differences.

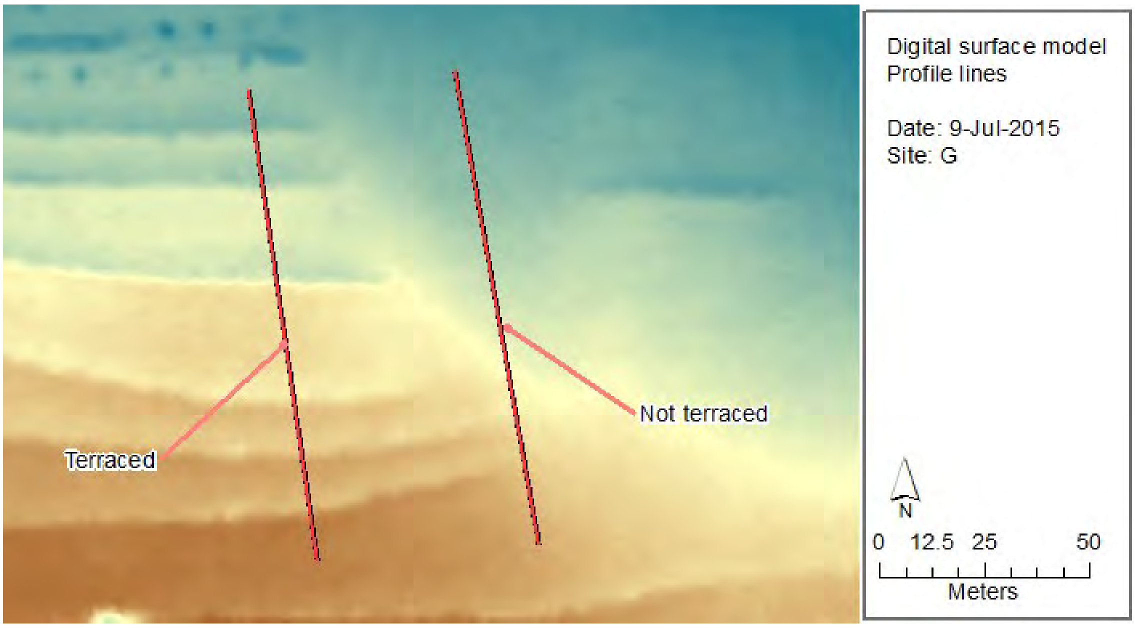

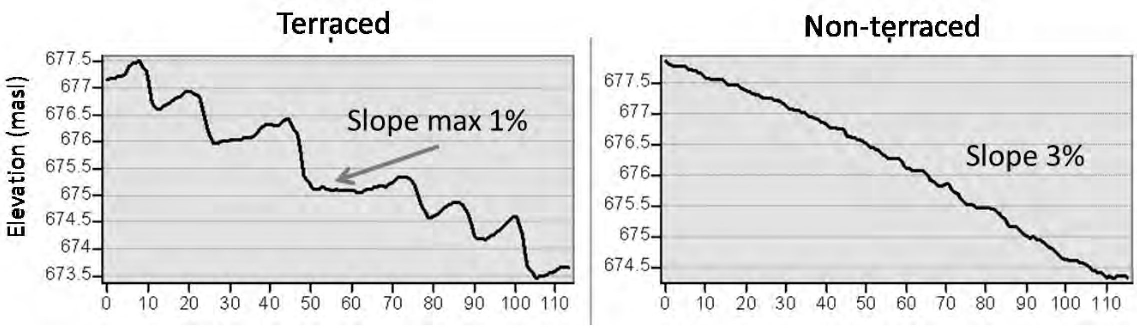

Figure 11. Comparison of slopes in a terraced and non-terraced similar area as obtained using Flying Sensors.

There is a wide variety of different terrace types, from forward-sloping terraces to level or backward-sloping bench terraces. To study how the terraces are sloped, the direction of the slope (aspect) can be calculated with sufficient detail to obtain insight in the type of terraces implemented in the area.

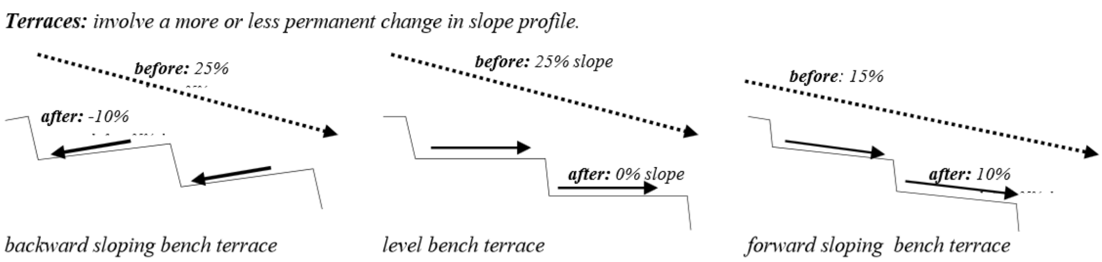

Figure 12. Different slope profiles for terraces (source: WOCAT questionnaire)

Figure 12 shows the direction of slope for an area where cereals are cultivated (left) with forward sloping terraces with large intervals, and on the right almonds with mixture of bench level terraces and backward sloping terraces.

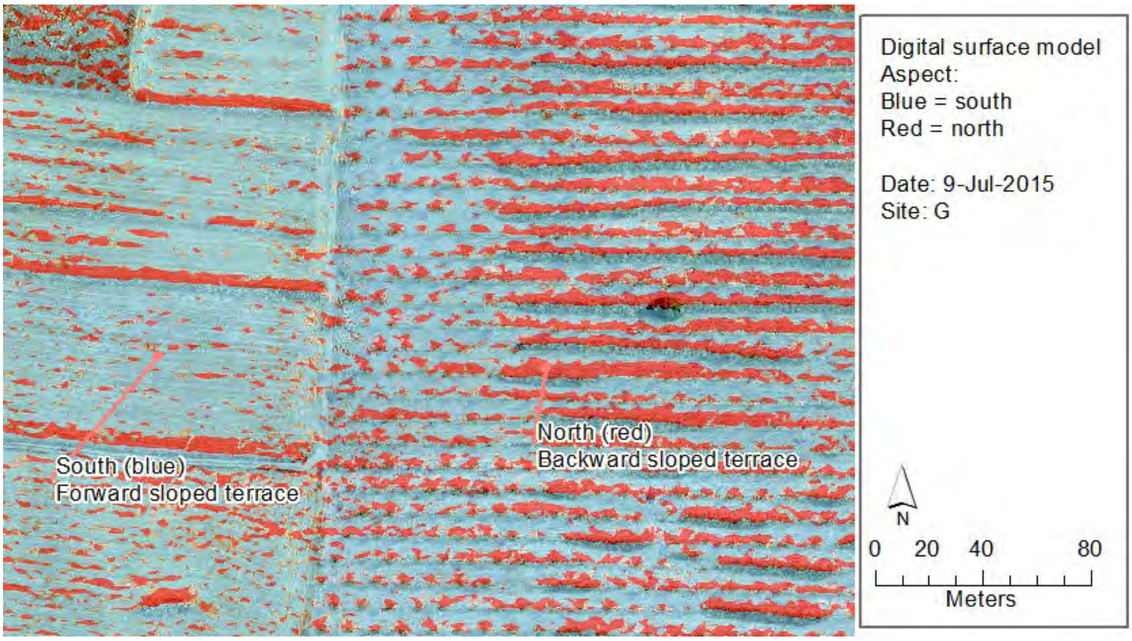

Figure 13. Aspect (slope direction) for an area where cereals are cultivated (left) with forward sloping terraces with large intervals, and on the right almonds with mixture of bench level terraces and backward sloping terraces.

6.3 Terrace intervals

Besides slope, strip width for vegetative strips and slope length for terraces (i.e. the terrace interval) are critical implementation factors. This is for example summarized in the USLE support practice factor P: based on field experiments standardized tables are available that relate these properties with a representative P factor value of the USLE equation. An example of such a table for contour stripcropping can be found in Table 1.

Table 1. USLE support practice P values for different for contour stripcropping (source: SWAT Input Manual Chapter 20)

Land slope (%)	P_{USLE} values[1]			Strip width (m)	Maximum length (m)
	A	B	C		
1 to 2	0.30	0.45	0.60	40	244
3 to 5	0.25	0.38	0.50	30	183
6 to 8	0.25	0.38	0.50	30	122
9 to 12	0.30	0.45	0.60	24	73
13 to 16	0.35	0.52	0.70	24	49
17 to 20	0.40	0.60	0.80	18	37
21 to 25	0.45	0.68	0.90	15	30

Figure 14 shows a terraced area, where a combination of imagery and a topographical index allows easy measuring of terrace interval (i.e. slope length). For larger areas, this can be automatized using GIS techniques.

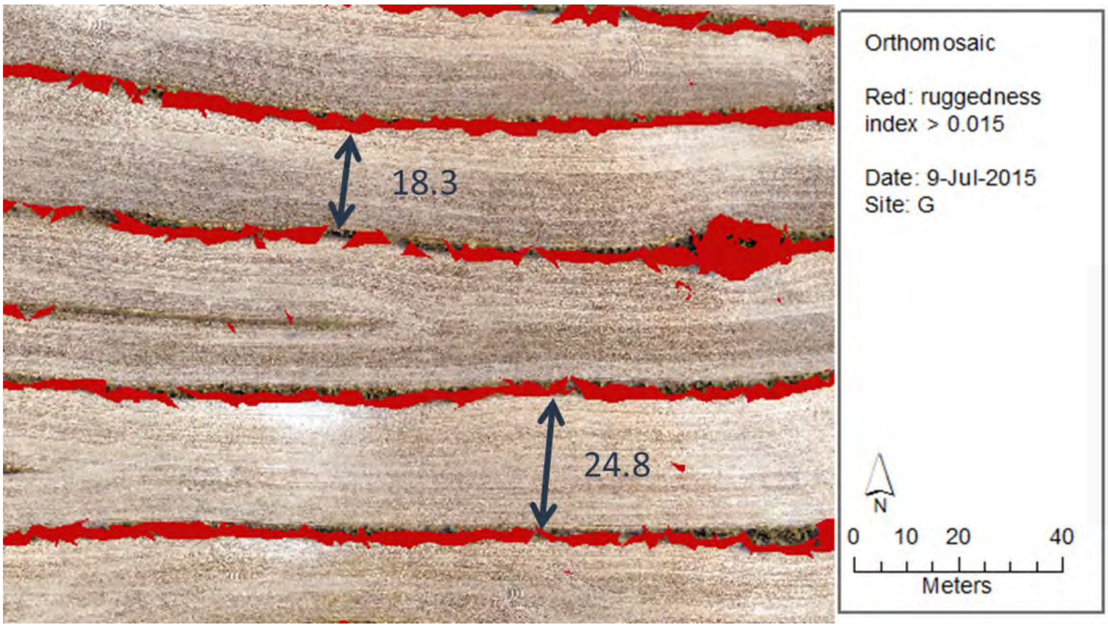

Figure 14. Slope length of a terraced area

6.4 Tillage

Many SLM technologies are based on the principle that farming should occur on the contour. This alone can reduce soil loss to approximately half of what it would be with cultivation up and down the slope. Contour ploughing is the farming practice of ploughing and/or planting across a slope following its elevation contour lines. These contour lines create a water break which reduces the formation of rills and gullies during times of heavy water run-off; which is a major cause of soil erosion. The water break also allows more time for the water to settle into the soil.

Figure 15 illustrates that using a combination of high-resolution imagery from Flying Sensors, and the high-resolution digital elevation model, it is relatively straightforward to identify whether ploughing occurs parallel to the contour lines or not. Clearly in this particular example the ploughing has been done perpendicular to the contour lines. This is not favourable as runoff velocities are likely to increase and rills will occur during rainfall events.

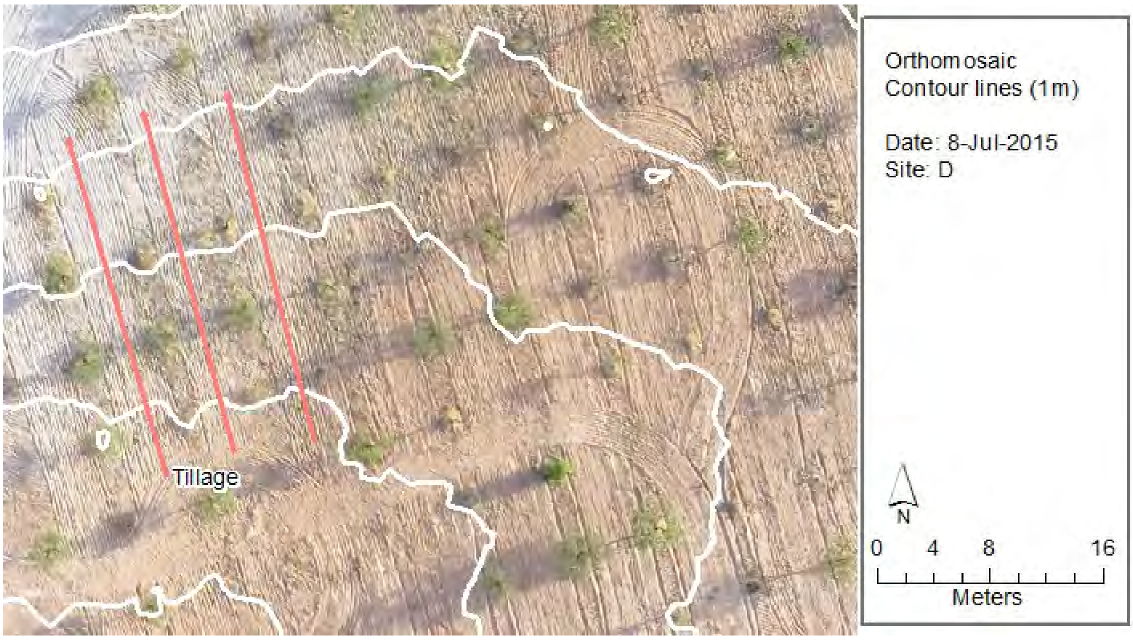

Figure 15. Tillage direction versus contour direction.

7 Monitoring Effectiveness of GWC Practices

Sustainable Land Management technologies can provide benefits to upstream farmers, and downstream actors in the basin that need a reliable source of water of good quality. Upstream benefits are related to agricultural productivity, and thus to soil fertility (soil organic matter) and water availability (soil moisture). A key benefiting sector downstream is irrigated agriculture, where Flying Sensor information can be used to monitor and optimize water use. Flying Sensors can provide detailed spatial information on stress factors and productivity.

Effectiveness upstream can also be monitored using multi-temporal imagery: changes in vegetative structure and elevation can reveal where the landscape has changed (e.g. fragmentation, productivity), where erosion sources and sinks are active. The information can also help quantifying the mobilization of sediments on those places where erosion is very localized and severe.

7.1 Soil Wetness Index

Based on the Flying Sensor digital elevation models, detailed hydrological information can be derived by using empirically-based indices or dynamic simulation models. A wide variety of soil wetness indexes can be derived, that use elevation data and a set of soil physical parameters. These wetness indexes rely often on discharge-contributing upslope area of each grid cell and the specific catchment area.

An example of a static soil wetness index is shown in Figure 16 (Saga Wetness Index). As can be seen, the areas above the stone walls are the areas that are likely to be wettest. In general the index suggests that they are wetter than other areas where flow concentrates and no stone walls are apparent.

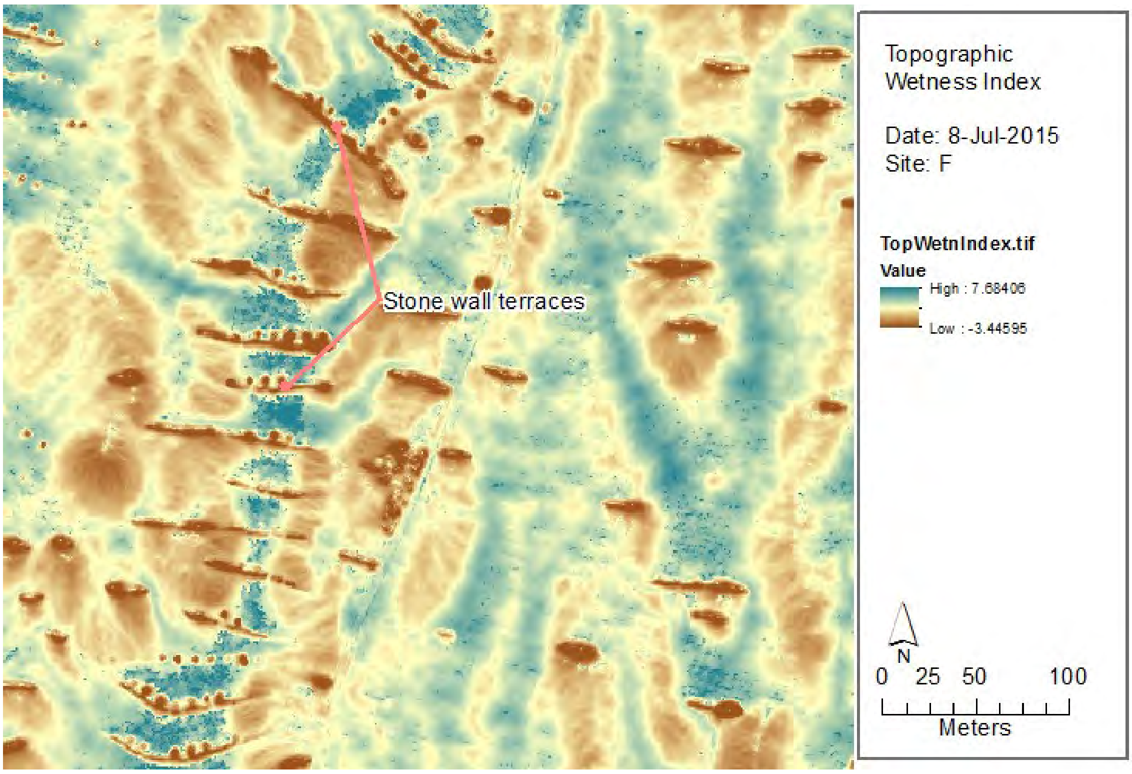

Figure 16. Soil Wetness Index for an area with stone walls of site F

This type of indices can be easily derived and are useful to study how the structural measures impact soil moisture. For more detailed quantitative estimates of soil moisture, the digital elevation model can be used as input in dynamic hydrological modelling.

7.2 Soil Organic Matter

The conservation of Soil Organic Matter (SOM) is one of the principle benefits of SLM technologies for farmers as it reduces the need for fertilizers and enhances agricultural productivity while simultaneously improving soil structure and stability against erosion and increasing the water holding capacity of the soil. It has been observed (e.g. WOCAT) that SLM technologies can increase Soil Organic Matter to higher values then levels before land cultivation. Monitoring this variable therefore can be very useful to measure the impact of conservation measures on farmer´s livelihoods.

Obtaining absolute estimates of SOM from remote sensing imagery is difficult as no generic relationships apply: reflections are dependent on many factors as soil type, soil wetness etc. However, monitoring gives a relative estimate of how SOM content changes after implementing soil conservation practices.

Soil organic matter has been related with high reflection in red, and low in green [*Melendez-Pastor et al.*, 2008]. As an example, the Normalized green-red difference index was calculated as it provides a standardized measure of the difference in reflections between red and green. It is defined as

$$NGRDI = \frac{G-R}{G+R}$$

Figure 17 shows the NGRDI index that was calculated from the optical imagery of the Flying Sensor at site F (same as in previous example for soil moisture) with the stone wall terraces. Low values of this index (brownish) are likely to correspond with high soil organic matter content.

Figure 17. Normalized Red-Green Difference Index based on visible imagery from Flying Sensor, as indicator for Soil Organic Matter content

7.3 Downstream water use

Water use and water stress in downstream irrigated areas can be monitored using Flying Sensors. Detailed spatial information on the status of irrigated crops can support farmers in increasing water productivity, detecting stress factors, and increasing the efficiency in water infrastructure.

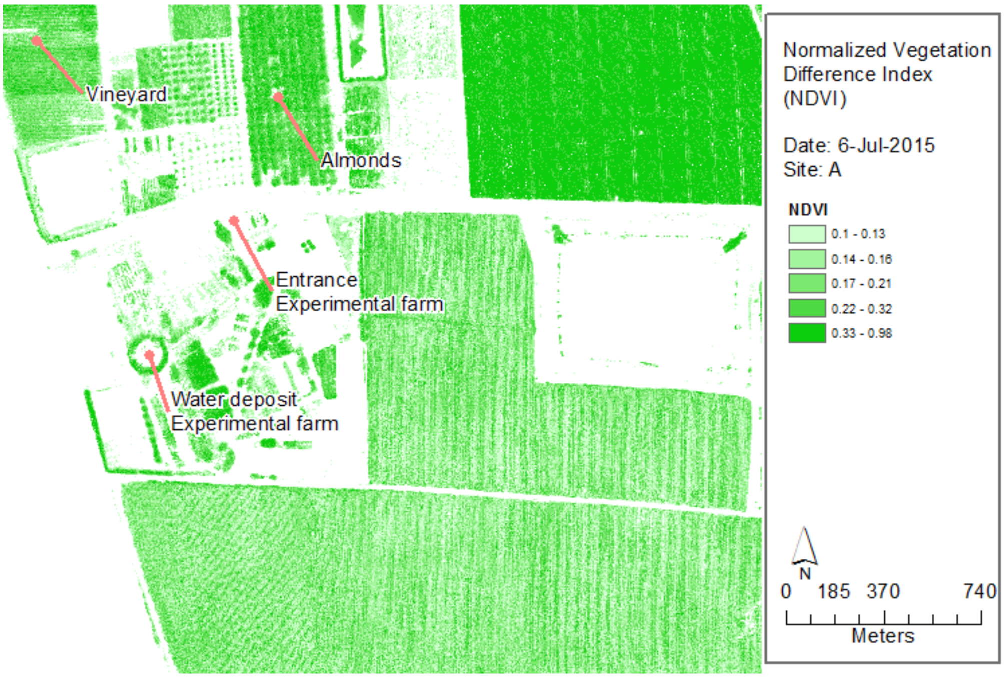

Figure 18. Vegetation greeness measured with NDVI for several irrigated crops

Figure 18 shows the Normalized Vegetation Difference Index (NDVI) for site A (experimental farm Tomás Ferro of the Universidad Politécnica de Cartagena, Spain). Different irrigated crops are cultivated within and around the farm. NDVI is dependent on crop type, cropping practices, and growth stage. The lowest NDVI values in this area can be found in the cereal plots.

From just the NDVI values it is hard to extract information on where the crop performs better in order to optimize farming practices (irrigation scheduling, fertilizers, pest management etc). Therefore, Figure 19 shows the NDVI anomaly per plot, calculated as:

$$Anomaly = \frac{NDVI_{pixel}}{NDVI_{plot\_average}}$$

Clearly some patterns can be observed in the cereal plots, probably related to soil properties and soil water content. In pepper, the tractor paths can be observed, but also some differences between the eastern and western part of the plot that may be related to water availability.

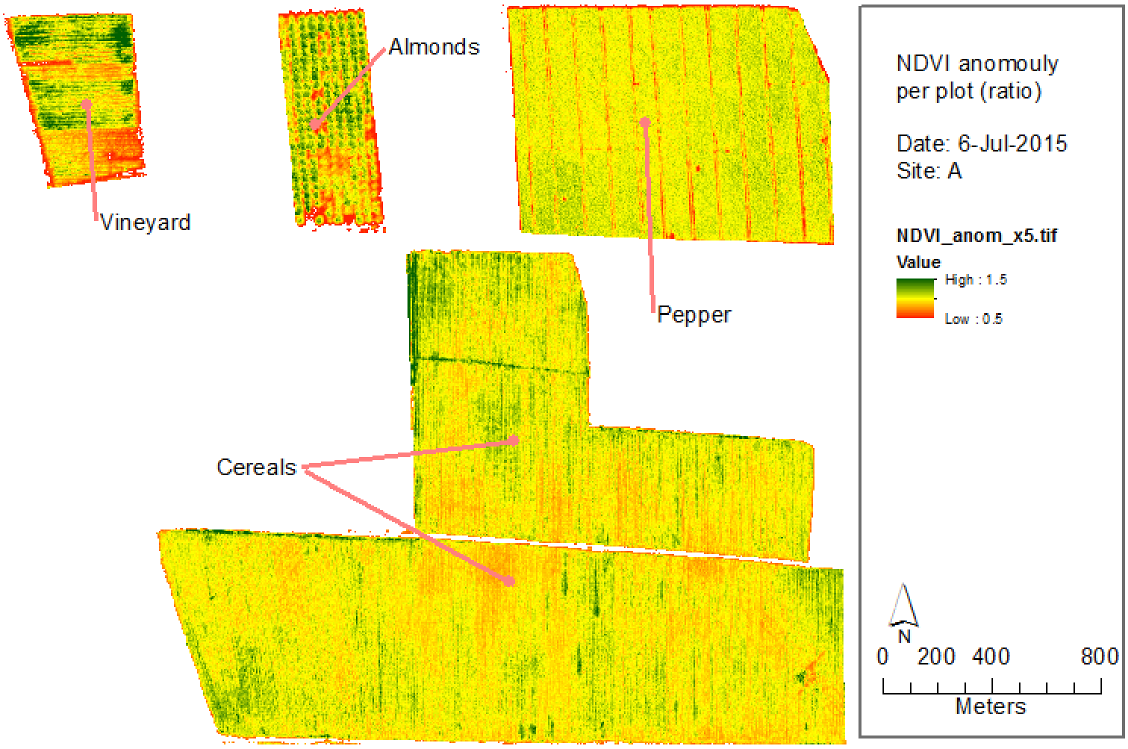

Figure 19. Anomalies for each plot in vegetation greenness (ratio-based) for several irrigated crops

For the irrigated almond trees and vineyard, Figure 20 shows a more detailed picture. For the vineyard, the image suggests that there are a few rows in the middle that are likely to receive less water. For the irrigated almond trees, which are part of the experimental farm, a clear anomaly is found in the area where regulated deficit irrigation is practiced.

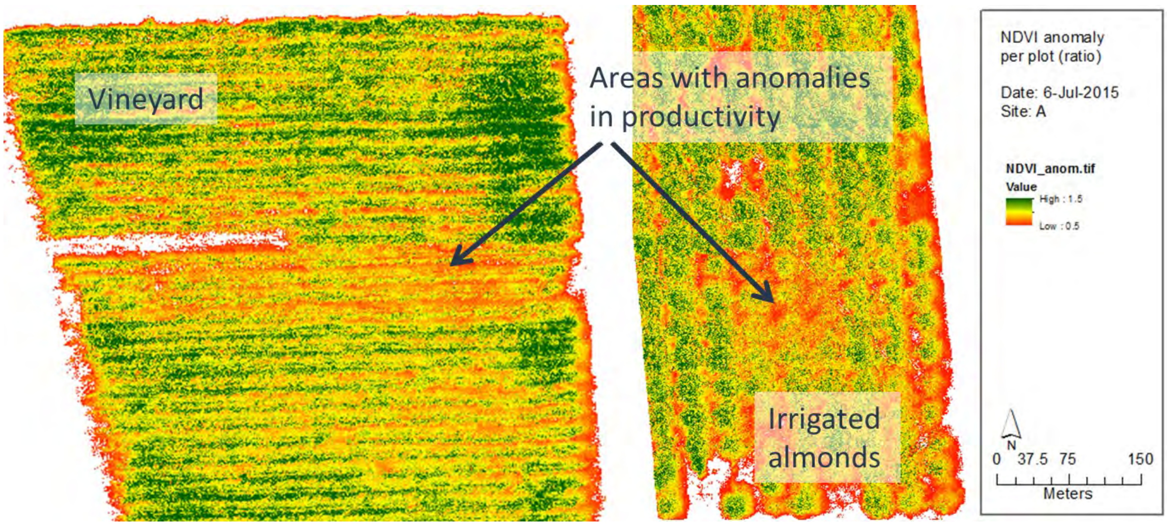

Figure 20. Detailed map of NDVI anomalies for vineyard and irrigated almond trees.

8 Recommendations

This report demonstrates how Flying Sensors can be used to support Green Water Credits monitoring. It provides preliminary guidance on the potential of this type of information for monitoring of farmers´ practices and supporting the implementation and operations of GWC.

Based on this preliminary study, the following recommendations are put forward for further analysis and guidance to monitor GWC implementation:

- The high resolution digital elevation models allow very precise analysis of topographical attributes that are relevant for measuring the implementation and effectiveness of practices. The terrain attributes and indices derived from these models allow quantifying better how different measures influence factors that are relevant for the productivity of upstream rainfed farming. A more in-depth study is recommended that takes full advantage of this high-resolution information to select useful terrain indicators to evaluate and benchmark GWC practices.
- From the visible and near-infrared imagery, relevant indicators can be obtained on vegetative status of the crops. This status is very much influenced by farming´s practices, as terraces, slopes, etc,. The available detailed information on vegetative status and terrain attributes can be used to better understand the link between practices and productivity.
- Another series of flights for the same sites can reveal how changes can be monitored. Digital elevation models can be compared to study changes due to erosion. Other relevant indices related to impacts (fragmentation, connectivity, soil organic matter, vegetation greenness) can be derived and compared with the first flight to assess the potential of this type of information for actual monitoring of changes due to farming practices.

9 References

Agisoft (2013), *PhotoScan Professional 0.9.1 User Manual*, St. Petersburg.

Fonstad, M. A., J. T. Dietrich, B. C. Courville, J. L. Jensen, and P. E. Carbonneau (2013), Topographic structure from motion: a new development in photogrammetric measurement, *Earth Surf. Process. Landforms*, *38*(4), 421–430.

Furukawa, Y., and J. Ponce (2009), Accurate Camera Calibration from Multi-View Stereo and Bundle Adjustment, *Int. J. Comput. Vis.*, *84*(3), 257–268.

Furukawa, Y., and J. Ponce (2010), Accurate, dense, and robust multiview stereopsis., *IEEE Trans. Pattern Anal. Mach. Intell.*, *32*(8), 1362–76.

Lowe, D. G. (2004), Distinctive Image Features from Scale-Invariant Keypoints, *Int. J. Comput. Vis.*, *60*(2), 91–110.

Lucieer, a., S. M. D. Jong, and D. Turner (2013), Mapping landslide displacements using Structure from Motion (SfM) and image correlation of multi-temporal UAV photography, *Prog. Phys. Geogr.*, *38*(1), 97–116, doi:10.1177/0309133313515293.

Melendez-Pastor, I., J. Navarro-Pedreño, I. Gómez, and M. Koch (2008), Identifying optimal spectral bands to assess soil properties with VNIR radiometry in semi-arid soils, *Geoderma*, *147*(3-4), 126–132, doi:10.1016/j.geoderma.2008.08.004.

Plets, G., W. Gheyle, G. Verhoeven, and J. De Reu (2012), Three-dimensional recording of archaeological remains in the, *Antiquity*, *86*, 884–897.

Snavely, N., S. M. Seitz, and R. Szeliski (2007), Modeling the World from Internet Photo Collections, *Int. J. Comput. Vis.*, *80*(2), 189–210.

Triggs, B., P. F. Mclauchlan, R. I. Hartley, and A. W. Fitzgibbon (2000), Bundle Adjustment — A Modern Synthesis, *Lect. Notes Comput. Sci.*, *1883*, 298–372.

Verhoeven, G. (2011), Software Review Taking Computer Vision Aloft - Archaeological Three-dimensional Reconstructions from Aerial Photographs with PhotoScan, *Archaeol. Prospect.*, *73*(18), 67–73.

WOCAT: World Overview of Conservation Approaches and Technologies (www.wocat.net)